J|A|C|S
ARTICLES
Published on Web 01/04/2006

Effect of Silicon Oxidation on Long-Term Cell Selectivity of Cell-Patterned Au/SiO_2 Platforms

Mandana Veiseh and Miqin Zhang*

Contribution from the Department of Materials Science and Engineering, University of Washington, Seattle, Washington 98195-2120

Received August 10, 2005; E-mail: mzhang@u.washington.edu

Abstract: Cellular patterning on silicon platforms is the basis for development of integrated cell-based biosensing devices, for which long-term cell selectivity and biostability remain a major challenge. We report the development of a silicon-based platform in a metal−insulator format capable of producing uniform and biostable cell patterns with long-term cell selectivity. Substrates patterned with arrays of gold electrodes were surface-engineered such that the electrodes were activated with fibronectin to mediate cell attachment and the silicon oxide background was passivated with PEG to resist protein adsorption and cell adhesion. Three types of oxide surfaces, i.e., native oxide, dry thermally grown oxide, and wet thermally grown oxide, were produced to illustrate the effect of oxide state of the surface on long-term cell selectivity. Results indicated that the cell selectivity over time differed dramatically among three patterned platforms and the best cell selectivity was found on the dry oxide surface for up to 10 days. Surface analysis results suggested that this enhancement in cell selectivity may be related to the presence of additional, more active oxide states on the dry oxide surface supporting the stability of PEG films and effectively suppressing the cell adhesion. This research offers a new strategy for development of stable and uniform cell-patterned surfaces, which is versatile for immobilization of silane-based chemicals for preparation of biostable interfaces.

I. Introduction

Significant advances have been made in development of bio-micro-electromechanical systems (Bio-MEMS), in which the materials and processing tools of microfabrication technology are used toward medical and bioanalytical applications.[1−3] Cell-patterned Bio-MEMS are powerful platforms for development of cell-based biosensors[4−6] and cell-based diagnostic, prosthetic, and therapeutic systems.[4,7,8] These systems are favored over in vitro protein-based, enzyme-based, or receptor-based systems because of their ability to detect many forms of substances, including chemical toxins, bacteria, and viruses[9−11] and provide insight into the physiological effect of an analyte. They are also favored over in vivo systems because it is often impossible to use human subjects for toxicological analysis.[7]

The success of cell-based systems hinges on our ability to develop microarrays of cells that can be easily integrated with microelectronics for rapid and accurate sample tests, which would greatly reduce the required sample volume, minimize contamination, and obtain high sampling throughput and reproducible data. Cell patterning can be achieved by tailoring surfaces to form distinct regions that have adhesive proteins or ligands to host one or groups of cells with a background inert to protein adsorption and cell adhesion. Cell patterning is commonly formed via soft lithography,[12] photochemistry,[13] or photolithography[14] techniques. In all of these techniques the patterns are formed either by generation of heterogeneous chemistry on a single material or by deposition of a second material in a certain shape and geometry followed by surface modification to form heterogeneous chemistry. The latter is the basis for cell-based biosensors in which the patterned regions are miniaturized arrays of metal electrodes such as gold and the background is a silicon-based material. The performance of these devices is strongly dependent on the long-term cell selectivity and biostability of the cell patterns upon their exposure to complex biological environments. We define cell selectivity as selective confinement of cells to the designated regions on substrates, usually a metal array. This can be achieved through application of a biostable and biocompatible surface-engineering scheme for both the cell adhesive and inert regions.

(1) Hanein, Y.; Pan, Y. V.; Ratner, B. D.; Denton, D. D.; Bohringer, K. F. *Sens. Actuators, B* **2001**, *81*, 49−54.
(2) Huang, Y.; Mather, E. L.; Bell, J. L.; Madou, M. *Anal. Bioanal. Chem.* **2002**, *372*, 49−65.
(3) Voskerician, G.; Shive, M. S.; Shawgo, R. S.; von Recum, H.; Anderson, J. M.; Cima, M. J.; Langer, R. *Biomaterials* **2003**, *24* (11), 1959−1967.
(4) Lin, H. J.; Charles, P. T.; Andreadis, J. D.; Churilla, A. M.; Stenger, D. A.; Pancrazio, J. J. *Anal. Chim. Acta* **2002**, *457* (1), 97−108.
(5) Pancrazio, J. J.; Gray, S. A.; Shubin, Y. S.; Kulagina, N.; Cuttino, D. S.; Shaffer, K. M.; Eisemann, K.; Curran, A.; Zim, B.; Gross, G. W.; O'Shaughnessy, T. J. *Biosens. Bioelectron.* **2003**, *18* (11), 1339−1347.
(6) Gray, D. S.; Tan, J. L.; Voldman, J.; Chen, C. S. *Biosens. Bioelectron.* **2004**, *19*, 1765−1774.
(7) Park, T. H.; Shuler, M. L. *Biotechnol. Prog.* **2003**, *19* (2), 243−253.
(8) Neumann, E.; Tonsing, K.; Siemens, P. *Bioelectrochemistry* **2000**, *51*, 125−132.
(9) DeBusschere, B.; Kovacs, G. T. *Biosens. Bioelectron.* **2001**, *16*, 543−556.
(10) Yicong, W.; Ping, W.; Xuesong, Y.; Gaoyan, Z.; Huiqi, H.; Weimin, Y.; Xiaoxiang, Z.; Jinghong, H.; Dafu, C. *Sens. Actuators, B* **2001**, *80*, 215−221.
(11) Pancrazio, J. J.; Whelan, J. P.; Borkholder, D. A.; Ma, W.; Stenger, D. A. *Ann. Biomed. Eng.* **1999**, *27*, 697−711.
(12) Xia, Y.; Whitesides, G. M. *Angew. Chem.* **1998**, *110* (5), 568−594.
(13) Tender, L. M.; Worley, R. L.; Fan, H. Y.; Lopez, G. P. *Langmuir* **1996**, *12*, 5515−5518.
(14) Knoll, W.; Liley, M.; Pisceivic, D.; Spinke, J.; Tarlov, M. J. *Adv. Biophys.* **1997**, *34*, 231−251.

The adhesive regions are normally composed of adsorbed, chemically bonded, or printed extracellular matrix (ECM) proteins that support cell adhesion.[15,16] The choices for inert regions vary to a large extent, i.e., from the masks that place a physical barrier on a modified surface[14] to physical and chemical surface modifications that tailor the surface inert.[17,18] They normally resist cell adhesion by blocking or reducing nonspecific protein interaction. Self-assembled monolayers (SAMs) that terminate in a short poly(ethylene glycol) (PEG) unit have been especially effective in this regard.[19] However, the properties of these surface coatings frequently deteriorate over time, due to either pinhole defects in the film or oxidation and decomposition of the PEG.[20,21]

We recently developed a highly selective and versatile surface molecular-engineering scheme for protein and cell patterning on Au/SiO_2 platforms.[18,22,23] However, the system tended to gradually lose cell selectivity after 1−2 days in culture. The present work pursues long-term cell selectivity and stability. We show that with our patterning technique the cell selectivity can be dramatically enhanced and prolonged by engineering the silicon surfaces to have proper oxidation states. This can be significant in engineering stable and controllable material−biosystem interfaces and in developing Bio-MEMS devices in general,[24] since almost all biomicrodevices inevitably involve the interactions of biomolecules with oxide surfaces of one type or another—whether formed naturally or created intentionally.

Three types of silicon surfaces that contained native oxide, dry thermally grown oxide, and wet thermally grown oxide, respectively, were produced as a basis for the inert regions of gold-patterned platforms. We name these surfaces as native oxide, dry oxide, and wet oxide for simplicity according to their oxide formation mechanisms. The gold-patterned substrates were then modified such that the silicon regions with native, dry, or wet oxide were reacted with a low molecular weight M-PEG-silane (M_w = 460−590 Da) to form inert (non-cell adhesive) coatings, and the gold electrodes were reacted with COOH-terminated thiols to covalently bind proteins to guide the subsequent cell adhesion. The surface chemical compositions of the substrates were characterized with X-ray photoelectron spectroscopy (XPS) before and after exposure to methoxy-PEG-silane (M-PEG). The wettability of PEG-treated surfaces was determined by contact angle measurements. Protein interaction with modified and unmodified surfaces was characterized by fluorescence microscopy. Long-term cell selectivity for cell patterning was monitored by differential interference contrast (DIC) reflectance microscopy for up to 10 days. The effect of oxide states of the surface on long-term cell selectivity and PEG stability was investigated by XPS.

II. Experimental Section

II.A. Materials. The following materials and chemicals were used as received: nanostrip 2X (Cyantek, Fremont, CA), 2-[methoxy-(polyethyleneoxy)propyl]trimethoxysilane (M_w = 460−590 Da) (Gelest, Morrisville, PA), Cy3 monoreactive NHS ester labels (Amersham Biosciences, Sweden), RPMI-1640 (ATCC, Manassas, VA), heat-inactivated fetal bovine serum (Invitrogen, Carlsbad, CA), penicillin−streptomycin (Gibco, Carlsbad, CA), 11-mercaptoundecanoic acid 95% (11-MUA), 3-mercaptopropionic acid 99% (3-MPA), *N*-hydroxysuccinimide 97% (NHS), 1-ethyl-3-(3-(dimethylamino)-propyl) carbodiimide (EDAC), fibronectin protein, trypsin-EDTA, sigmacote, and glutaraldehyde (Sigma-Aldrich, Milwaukee, WI). All the solvents including toluene and triethylamine were HPLC grade and were purchased from Aldrich (Milwaukee, WI). Absolute ethanol was always deoxygenated by dry N_2 before use.

II.B. Substrate Preparation. Four inch p-type silicon substrates of (100) orientation were cleaned with piranha (hydrogen peroxide/sulfuric acid 2:5 v/v) at 120 °C for 10 min, dipped in HF, and rinsed with DI water thoroughly. A layer of positive photoresist (1.1 μm) was then coated on the surface, and an array of squares (20 μm × 20 μm) was patterned on the substrate upon exposure to UV light through a mask. A thin layer of titanium (Ti) of 10 nm in thickness was then deposited onto the photoresist-developed substrate at a deposition rate of 0.3 Å/s. Gold films of 100 nm in thickness were subsequently deposited on the Ti at a deposition rate of 5 Å/s. The photoresist was dissolved in acetone, and the remaining metal films were lifted off. The surface with native oxide was formed as a result of exposure of the substrates to the air. The surface with dry oxide was created by additionally exposing the surface to buffered oxide etch (HF/NH4F 5:1 v/v) for 60 s and rinsing with DI water to remove the native oxide on silicon regions, followed by flushing with a dry oxygen flow for 6 h at 400 °C, yielding a 60 Å oxide layer on the silicon regions. The surface with wet oxide was prepared following the same procedure except that the substrates were placed under a wet oxygen flow at 850 °C, yielding a 1000 Å oxide layer on the silicon regions. The gold-patterned silicon oxide wafers were cut into 8 mm × 8 mm slides. To minimize surface contaminants and unexpected scratches, the silicon oxide wafers were coated with a layer of photoresist of 2 μm in thickness on their polished sides before cutting.

II.C. Surface Engineering. II.C.1. Silicon Substrates. Silicon substrates were washed with acetone, ethanol, and DI water before being placed in nanostrip 2X at room temperature for 30 min, followed by an extensive rinse with DI water and passive drying under nitrogen. The substrates were then reacted with M-PEG-silane according to the following procedure. The M-PEG-silane solution was prepared in nitrogen-filled reaction flasks by adding 3 mM PEG-silane in anhydrous toluene containing 1% triethylamine as catalyst. The PEG reaction proceeded under nitrogen at 60 °C for 18 h. Loosely bound moieties were removed from the PEG-treated surfaces by sonicating them in toluene and ethanol for 5 min each, followed by rinsing with DI water and drying under nitrogen.

II.C.2. Gold-Patterned Silicon Substrate. The gold regions of the piranha-treated substrates were first reacted with a 20 mM mixture of alkane thiols of 11-mercaptoundecanoic acid (MUA) and 3-mercapto-propionic acid (MPA) (1:10 v/v) for 16 h to form a self-assembled monolayer (SAM). The silicon background was passivated with PEG through the procedure described above. The substrates were then immersed in an aqueous solution of 150 mM EDAC and 30 mM *N*-hydroxysuccinimide (NHS) for 30 min to attach the NHS group to the −COOH terminus of SAM. The substrates with NHS on the gold and PEG on the silicon oxide were sterilized with 70% ethanol for 15 min and exposed to fibronectin protein at a concentration of 0.1 mg mL^{-1} in a phosphate buffer solution (PBS) of pH = 8.2 at room temperature for 45 min. To remove loosely bound moieties after each step of the surface modification, the substrate was rinsed with its original solvent and DI water, respectively. As a result, the immobilized protein

(15) Pirone, D. M.; Chen, C. S. *Journal of Mammary Gland Biology and Neoplasia* **2004**, *9* (4), 405−417.
(16) Flaim, C. J.; Chien, S.; Bhatia, S. N. *Nat. Methods* **2005**, *2* (2), 119−125.
(17) Nelson, C. M.; Raghavan, S.; Tan, J. L.; Chen, C. S. *Langmuir* **2003**, *19* (5), 1493−1499.
(18) Veiseh, M.; Wickes, B. T.; Castner, D. G.; Zhang, M. *Biomaterials* **2004**, *26* (16), 3315−3324.
(19) Mrksich, M. *Curr. Opin. Chem. Biol.* **2002**, *6* (6), 794−797.
(20) Nuzzo, R. G. *Nat. Mater.* **2003**, *2* (4), 207−208.
(21) Mrksich, M. *Chem. Soc. Rev.* **2000**, *29* (4), 267−273.
(22) Veiseh, M.; Zareie, M. H.; Zhang, M. Q. *Langmuir* **2002**, *18* (17), 6671−6678.
(23) Lan, S.; Veiseh, M.; Zhang, M. *Biosens. Bioelectron.* **2005**, *20*, 1697−1708.
(24) Bashir, R. *Adv. Drug Delivery Rev.* **2004**, *56*, 1565−1586.

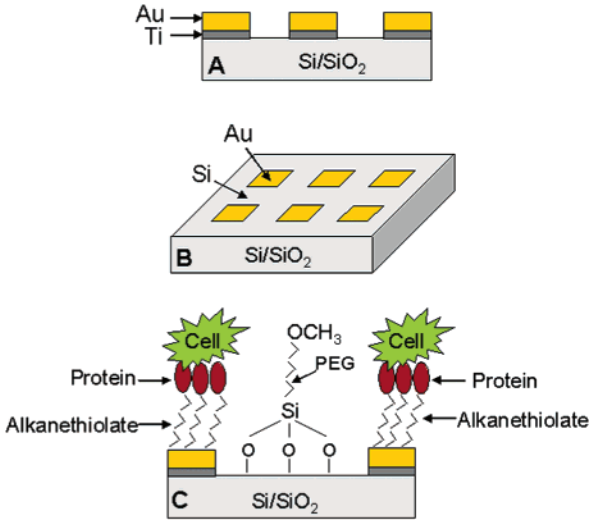

Figure 1. Schematic representation of the surface modification scheme for guided cell adhesion on gold-patterned surfaces. (A) Side view of the microfabricated substrate. (B) Top view of the gold-electrode-patterned substrate. (C) Side view of a surface-engineered substrate: the gold array coated with alkanethiolate SAMs and covalently bound with fibronectin proteins to mediate cell adhesion; the silicon regions passivated with M-PEG-silane.

formed a robust biocompatible layer on the gold arrays, and the M-PEG-silane formed an inert, biocompatible layer on the silicon oxide background. The chemical scheme of this surface molecular engineering is shown in Figure 1.

II.D. Fluorescence Labeling of Proteins. Fibronectin (M_w = 440 kDa) at a concentration of 1 mg/mL in PBS (pH 8.3) was reacted with Cy3 monoreactive NHS ester (M_w = 765.95 Da, 10 mg/mL in dimethylformamide) at a 100:1 ratio of dye to protein. The reaction proceeded in the dark for 30 min at room temperature with gentle stirring every 10 min. The unconjugated dye was separated by dialysis against PBS overnight at 4 °C using a Slide-A-Lyzer (Pierce Biotechnology, IL) membrane (exclusion limit of M_r = 3500). Samples were diluted with PBS to a 0.1 mg/mL concentration, verified with UV spectroscopy before application to the surfaces. The UV absorbance of the solution diluted 4-fold was 0.40225 and 1.974 AU at 280 and 548 nm, respectively. Considering a molar extinction coefficient of 150 000 M^{-1} cm^{-1} for Cy3 dye and 563 200 M^{-1} cm^{-1} for fibronectin, a labeling ratio of 30.33 ([Cy3]/[fibronectin]) was detected.

II.E. Cell Culture. Mouse macrophage (RAW 264.7) cell line was cultured in 75 cm^2 flasks at 37 °C in a humidified atmosphere with 5% CO_2. The medium contained 10% fetal bovine serum (FBS) in RPMI-1640 supplemented with 2 mM L-glutamine, 50 IU mL^{-1} penicillin, and 50 μg mL^{-1} streptomycin. The medium was changed every third day. For cell adhesion, 0.5 mL of macrophage cells at a concentration of 2 × 10^5 cells mL^{-1} was plated onto the protein-patterned substrates. The cells were allowed to adhere for 3, 7, and 10 days under the standard culture condition. The adhered cells were fixed with 2% glutaraldehyde for 20 min at room temperature.

II.F. Instrumentation. II.F.1. X-ray Photoelectron Spectroscopy (XPS). XPS spectra were taken on a Surface Science Instruments S-probe spectrometer. This instrument has a monochromatized Al Kα X-ray source. The X-ray spot size for these acquisitions was on the order of 800 μm. Pressure in the analytical chamber during spectral acquisition was less than 5 × 10^{-9} torr. The pass energy for survey spectra (composition) was 150 eV, and that for high-resolution C_{1s} (HRC) and Si_{2p} (HRSi) scans was 50 eV. The takeoff angle (the angle between the sample normal and the input axis of the energy analyzer) was 55° (≅ 50 Å sampling depth).

The Service Physics ESCAVB Graphics Viewer program was used to determine peak areas, calculate the elemental compositions from peak areas, and peak-fit the high-resolution spectra. The binding energy scale of the high-resolution C_{1s} spectra was calibrated by assigning the hydrocarbon peak in the C_{1s} high-resolution spectrum a binding energy of 285.0 eV. The binding energy scale for the Si_{2p} high-resolution spectra was calibrated to the C_{1s} peak position in the survey scan.

II.F.2. Contact Angle Measurements. Contact angles were measured by the sessile drop technique using a Rame-Hart 100 goniometer under ambient laboratory conditions (~40% humidity). A 2 μL drop of distilled water was applied to the surface, and the contact angle measurements were made within 30 s of the contact. The measurements were repeated for five samples.

II.F.3. Differential Interference Contrast (DIC) Reflectance Microscopy. Cell-patterned surfaces were characterized with a differential interference contrast (DIC) reflectance microscope (Nikon E800 Upright Microscope, New York, NY). Surfaces were visualized using a DIC-10× (N. A. 0.3) and DIC-50× (N. A. 0.8) objectives. Images were acquired by a Coolsnap camera (series A99G81021, Roper scientific Inc, AZ) attached to the microscope and a computer.

II.F.4. Fluorescence Microscopy. Fluorescence images were acquired on a Nikon Eclipse E800 upright wide field fluorescent microscope (Nikon Instruments, Inc., Melville, NY) equipped with a Photometrics CoolSNAP HQ CCD camera (Roper Scientific, Inc., Tucson, AZ). Surfaces were visualized using a DIC-10× (0.46) objective and rhodamine filter (excitation, 530−560 nm; emission, 590−650 nm). The amount of proteins adsorbed on surfaces was quantified by fluorescence intensity measurements. To avoid the interference from gold electrodes, the substrates without gold patterns were used. A rectangular region of interest (ROI) was selected on each image, and intensity per area was calculated and presented in arbitrary units.

III. Results and Discussion

III.A. X-ray Photoelectron Spectroscopy (XPS). High-resolution XPS spectra were acquired on the solid silicon substrates before and after surface modification with methoxy-PEG-silane (M-PEG). The results are shown in Figure 2.

The native oxide substrate showed the expected binding energy of elemental silicon (~99.7 eV) and SiO_2 (~103.5 eV). The dry oxide surface showed a similar spectrum as that of native oxide but with an asymmetric peak at ~102 eV, indicating the presence of a different silicon oxide state than those present on the native and wet oxide surfaces. This additional oxide state corresponds to silicon oxidation states ($SiO_{x<2}$) other than SiO_2. A similar finding was observed by Kandilioti et al. at a binding energy of 101.3 eV for silicon oxide at other oxidation states.[25] These are more chemically active states than those of SiO_2 and may play an important role in cell selectivity on our patterned surfaces as shown later. The wet silicon oxide surface had only a SiO_2 peak in its XPS spectrum indicating that the silicon background was completely covered by silicon dioxide.

Survey spectra indicated an increase in the carbon content and a decrease in the silicon content on all of the PEG-modified surfaces compared to that of their unmodified counterparts (data not shown). More oxygen was observed on both native and dry oxide after PEG modification, as opposed to wet oxide surfaces. The decreased amount of oxygen on the wet oxide was due to the fact that the wet oxide surface was mainly composed of silicon dioxide before PEG modification.

Table 1 represents the high-resolution XPS analyses of the Si_{2p} components on the oxide surfaces and the C_{1s} components on the PEG-modified surfaces. The spectra of high-resolution

(25) Kandilioti, G.; Siokou, A.; Papaefthimiou, V.; Kennou, S.; Gregoriou, V. G. *Appl. Spectrosc.* **2003**, *57* (6), 628−635.

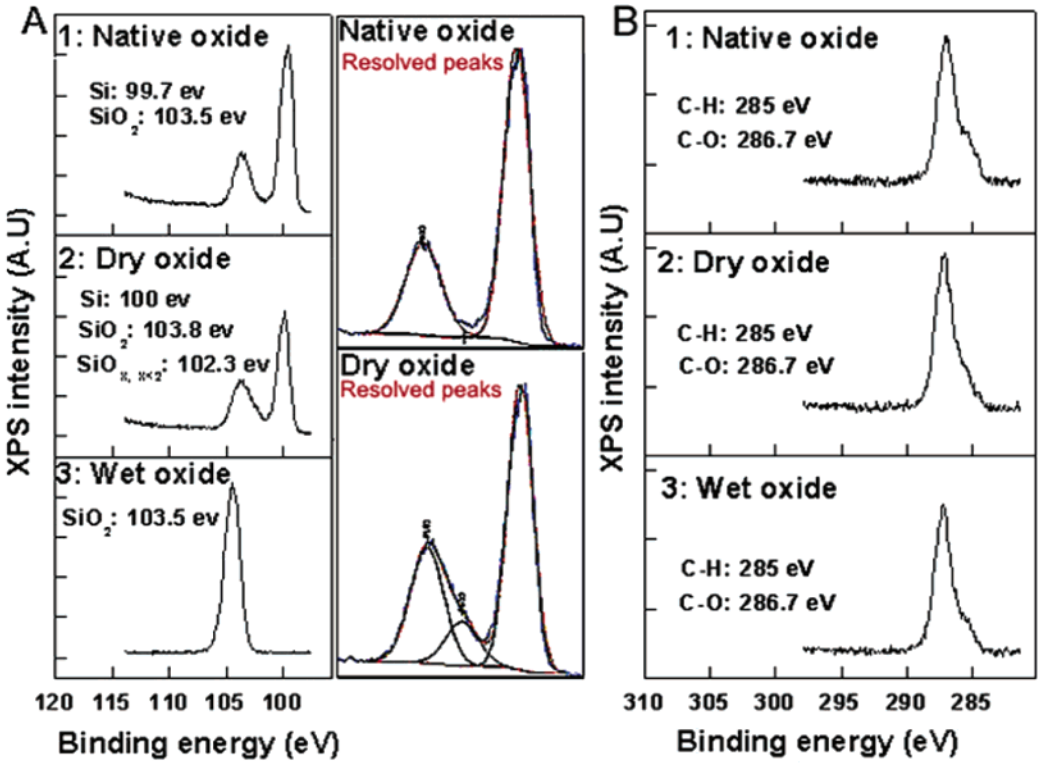

Figure 2. (A) High-resolution Si_{2p} spectra of silicon substrates coated with (1) native oxide, (2) dry oxide, and (3) wet oxide. (B) High-resolution C_{1s} spectra of PEG on silicon substrates coated with (1) native oxide surface, (2) dry oxide surface, and (3) wet oxide.

Table 1. High-Resolution XPS Si_{2p} and C_{1s} Analyses for Chemical Compositions[a]

(A) sample	% composition Si	$SiO_{x<2}$	SiO_2	(B) sample	% composition C–H	C–O	C═O
native oxide	69.64		30.36	Native oxide	15.1	80.6	4.3
dry oxide	58.45	11.85	29.7	dry oxide	14.8	82	3.2
wet oxide			100	wet oxide	15	79.7	5.3

[a] Spectra were taken at a 55° takeoff angle from (A) silicon oxide substrates and (B) PEG-modified silicon oxide substrates. The percentages are atomic percents of each type of surface atom calculated from survey spectra scan (Figure 2).

C_{1s} for all PEG-modified surfaces appeared to be similar, and the amounts of PEG on them were about the same. Further elaborations on the PEG component analysis are presented in the following sections.

III.B. Contact Angle Measurements on Silicon Surfaces. Water contact angles on all three types of silicon surfaces were measured after the surfaces were modified with PEG. The contact angle values of the three surfaces (native oxide, 31.6 ± 1.34°; dry oxide, 29.8 ± 0.83°; wet oxide, 30.4 ± 2.4°) are very similar and in agreement with those reported in the literature for such surface treatments.[26−28]

Despite the apparent differences in the nature of silicon oxide layers grown on the three surfaces before M-PEG-silane modification, both the contact angle measurements and XPS data indicated that about the same amount of PEG was coated on all three surfaces.

III.C. Protein Interaction with Surfaces. Protein adsorption on the gold-patterned surfaces was visualized with fluorescence microscopy on both unmodified (clean Au/SiO_2) surfaces and the surfaces modified with SAM on gold and PEG on silicon oxide as described above (Figure 1). The surfaces were exposed to fibronectin−Cy3 conjugate immediately following the surface modification. Figure 3 shows fluorescent images of the unmodified (left panel) and modified (right panel) surfaces with the silicon background immobilized with native oxide (A and B), wet oxide (C and D), and dry oxide (E and F). For the unmodified surfaces, proteins were randomly adsorbed over both the Au and silicon oxide regions (images A, C, and E), and particularly, the surface with wet oxide was heavily covered with proteins with no electrodes visible. The results reveal the influence of the silicon oxide state on protein adsorption.

After surface modification, the protein was selectively adsorbed on gold electrodes of all three surfaces (B, D, and F). However, a slight nonspecifically adsorbed protein was seen on the silicon region of the wet oxide surface (D). This phenomenon can be attributed to the strong affinity of the wet oxide for protein adsorption (C). This high affinity makes the wet oxide surface more susceptible to the defects presented in the PEG coating in preventing protein adsorption than the other surfaces, resulting in a high local protein adsorption (and subsequent cell adhesion when exposed to cells) on defected sites. In contrary, the PEG-modified dry oxide surface is expected to have higher protein resistance. Quantitative measurements of fluorescence intensities of the silicon surfaces yielded the following: wet oxide, 60; native oxide, 17; and dry oxide, 11, from the unmodified surfaces. This indicates that the dry oxide layer on the silicon region is the least biofouling layer by itself, and thus, the order of possible biofouling appeared to be: dry oxide < native oxide < wet oxide.

III.D. Cell Selectivity on Gold-Patterned Substrates. Cell selectivity was studied by culturing murine macrophage cells

(26) Papra, A.; Gadegaard, N.; Larsen, N. B. *Langmuir* **2001**, *17*, 1457−1460.
(27) Alcantar, N. A.; Aydil, E. D.; Israelachvili, J. N. *J. Biomed. Mater. Res.* **2000**, *51*, 343−351.
(28) Jo, S.; Park, K. *Biomaterials* **2000**, *21* (6), 605−616.

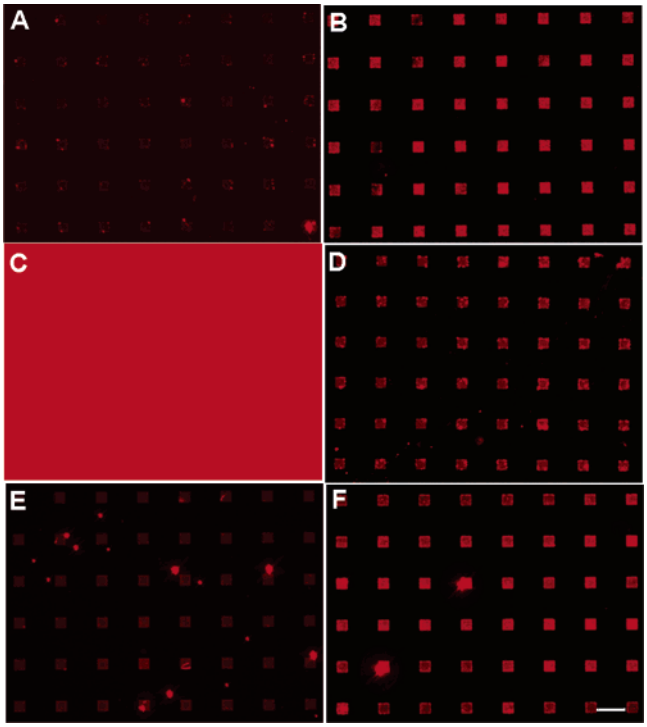

Figure 3. Fluorescent images of the fibronectin−Cy3 conjugate adsorbed on the unmodified (left panel) and PEG-modified (right panel) surfaces patterned with gold electrodes and with native oxide (A and B), wet oxide (C and D), and dry oxide (E and F) on a silicon background. The scale bar is 60 μm.

on the patterned substrates and monitored for up to 10 days (a typical time period for practical applications of cell-based biosensors). Cell selectivity was defined as selective confinement of cells to the designated regions—the gold arrays of electrodes in this case. Macrophage was used as the model cell line for cell selectivity study because of its important physiological functions in the human body.[29,30] For example, they have potentials for use as cellular delivery vehicles for gene therapy of diseased tissues and are an important source of mitogenic growth factors and proangiogenic cytokines in wound healing.[31,32] Selective suppression of macrophage activation is also a possible approach to diminishing local inflammation.[29,33] Combined with ink jet or other analyte-positioning techniques, surfaces patterned with macrophages may be used as sensing arrays for rapid detection of a variety of external stimuli and screening of drugs.

DIC reflective images were acquired after 2 days of cell culture and up to 10 days, since all of the surfaces had formed a uniform and highly selective cell pattern up to 1 day during which time no apparent difference on cell morphology was observed. These results are shown in Figure 4. Images were acquired on day 3, 7, and 10 (presented horizontally from left to right over time). Images A−C, D−F, and G−I are the substrates with native oxide, wet oxide, and dry oxide, respectively.

It is seen that the cell selectivity over time differed dramatically among the three patterned platforms. Cells started to migrate to the background on the native oxide surface on day 3 (image A), and the patterned surface completely lost cell selectivity on day 10 (image C). The wet oxide surface (images D−F) has much better cell selectivity than the native oxide surface, and the dry oxide surface (images G−I) shows very high cell selectivity through the duration of the study (10 days). Dry oxide has an additional advantage of being a better insulator,[25] which would enhance the performance of cell-based biosensors by increasing the electrical signal-to-noise ratio.

The prolonged cell selectivity on the dry oxide surface might be related to the intermediate oxidation state for the silicon (Table 1A). This is a more chemically reactive state than a fully stable SiO_2 and may result in different types of reactions. It has been reported[34] that methyl trimethoxy silanes react directly with dehydroxylated silica surfaces to form stable, chemically bound alkylsiloxanes and alkoxides at 330 K. Dubois et al.[34] have shown that model silane coupling agents can react directly with the highly strained siloxane bonds present on dehydroxylated silica without the involvement of surface hydroxyl groups. They also showed that trimethoxy silanes that are strongly bonded on surfaces at 330 K are extremely thermally stable. The fact that the PEG used for this study was a trimethoxy silane-PEG and was reacted with the surface at ~333 K may justify the observed behavior of the dry oxide surface. Thus, the interaction of PEG with the active state of silicon oxide might have contributed to formation of a more stable PEG coating on the silicon substrate.

To validate this viewpoint, the stabilities of the PEG coatings on three model surfaces under cell culture condition were assayed using serum-containing medium. PEG-modified surfaces were incubated in the medium at 37 °C and 5% humidity, and XPS analysis was performed on the samples on day 0, 3, 7, and 10. The results are shown in Table 2.

Most noticeable is the appearance of the O−C═O peak at ~289 eV on all the surfaces after 3 days of cell culture. This can be attributed to the partial oxidation of PEG in the cell culture medium. The amount of O−C═O was maximum on the native and wet oxide and minimum on the dry oxide surfaces through the period of study. The change in this peak provides an indication of the PEG oxidation level over time but does not rule out the possibility of PEG decomposition or degradation. PEG degradation can be estimated by the change in the amount of C−O over time. In this context, the degradation rate is defined as $\Delta CO_t/CO_0 = (CO_0 - CO_t)/CO_0$, where CO_0 and CO_t represent the amount of C−O initially and at time t, respectively. A high $\Delta CO/CO_0$ value corresponds to a high degradation rate. The results calculated from data in Table 2 are shown in Table 3.

PEG on the native oxide surface showed a considerable degradation on day 3 ($\Delta CO/CO_0 = 0.719$). The PEG degradation proceeded much slower on the dry oxide and wet oxide surfaces ($\Delta CO/CO_0 = 0.036$ and 0.035, respectively). PEG on the both types of surfaces remained stable up to 7 days and was partially degraded afterward. PEG on dry oxide had the least degradation for up to 10 days. When this result is compared with the cell-patterning images shown in Figure 4, a marked consistency is seen: the cell selectivity over time is directly

(29) Kao, W. J.; Hubbell, J. A.; Anderson, J. M. *J. Mater. Sci.: Mater. Med.* **1999**, *10* (10−11), 601−605.
(30) Pearsall, N. N.; Weiser, R. S. *The Macrophage*; Lea & Febiger: Philadelphia, PA, 1970.
(31) Kirsh, R.; Bugelski, P. J.; Poste, G. *Ann. N.Y. Acad. Sci.* **1987**, *507*, 141−154.
(32) Burke, B.; Sumner, S.; Maitland, N.; Lewis, C. E. *J. Leukocyte Biol.* **2002**, *72*, 417−428.
(33) Collier, T. O.; Thomas, C. H.; Anderson, J. M.; Healy, K. E. *J. Biomed. Mater. Res.* **2000**, *49* (1), 141−145.
(34) Dubois, L. H.; Zegarski, B. R. *J. Phys. Chem.* **1993**, *97*, 1665−1670.

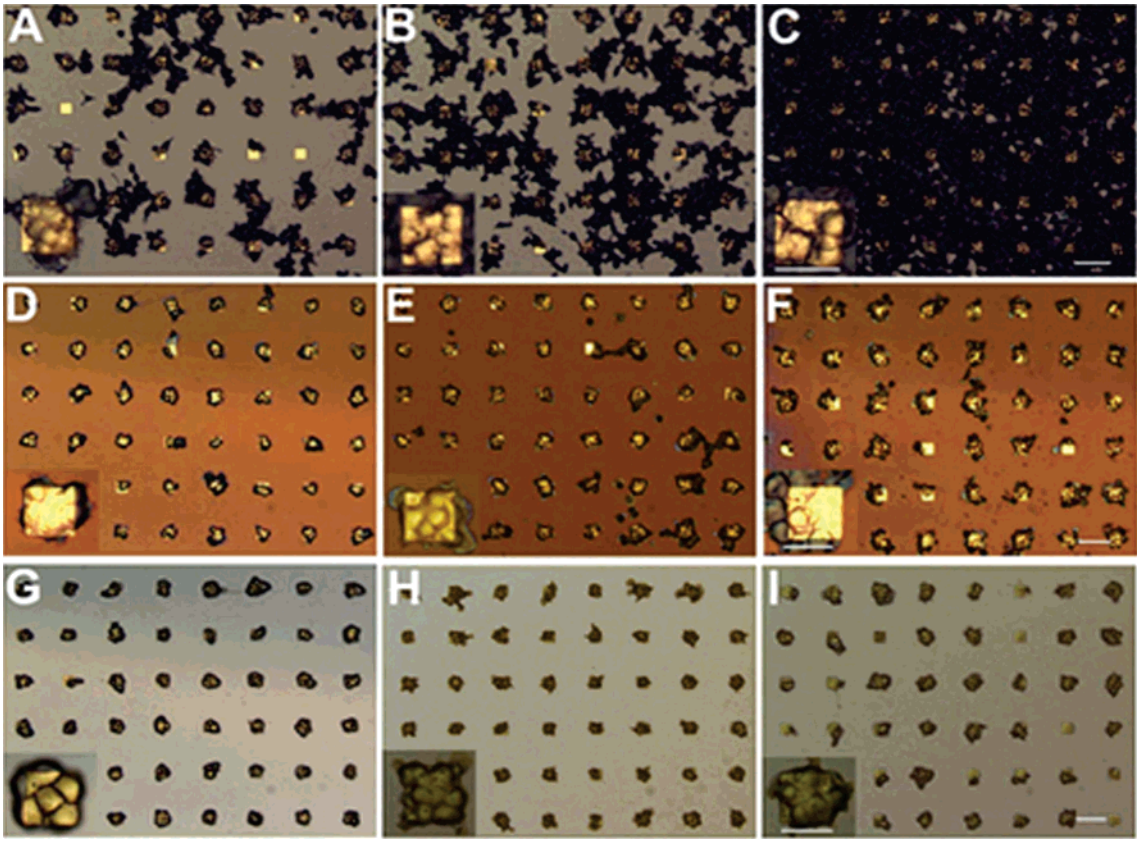

Figure 4. DIC reflectance microscopic images of macrophage cells cultured on gold-patterned silicon surfaces up to 10 days. Images A−C: surfaces with native oxide on silicon background. Images D−F: surfaces with wet oxide on silicon background. Images G−I: surfaces with dry oxide on silicon background. Cell culture time: 3, 7, and 10 days from left to right. Scale bars are 60 μm in all low-magnification images and 20 μm in all high-magnification images (insets in all images).

Table 2. High-Resolution XPS C_{1s} Analysis of Chemical Compositions of PEG-Modified Substrates[a]

	% composition											
	day 0			day 3			day 7			day 10		
sample	C–H ~285	C–O ~287	C=O ~288	C–H ~285	C–O ~287	O–C=O ~289	C–H ~285	C–O ~287	O–C=O ~289	C–H ~285	C–O ~287	O–C=O ~289
PEG-native	15.1	80.6	4.3	72.0	22.6	5.4	72.7	22.3	5	70.8	21.9	7.3
PEG-dry	14.8	82	3.2	19.1	79.0	1.9	20.1	78.1	1.8	37	60.7	2.3
PEG-wet	15	79.7	5.3	17.9	76.9	5.2	22.3	72	5.7	49.8	46	4.2

[a] Spectra were taken at 55° takeoff angle, after the substrates were incubated in cell culture medium for 3, 7, and 10 days.

Table 3. Time-Dependent Degradation Rate of the PEG Coatings on Gold/Silicon Oxide Substrates in Cell Culture Medium at 37 °C and 5% Humidity

	degradation rate $(CO_0 - CO_t)/CO_0$		
sample	PEG-native	PEG-dry	PEG-wet
day 3	0.719	0.036	0.035
day 7	0.723	0.047	0.096
day 10	0.728	0.259	0.422

correlated to PEG degradability. Thus, maintaining PEG integrity over time, particularly in cell culture medium as far as ligand-mediated cell patterning is concerned, is a key to the success of prolonged cell selectivity and biostability. This was achieved in this study by engineering the silicon surface to change its native oxidation state, on which a more stable PEG coating was obtained.

IV. Conclusions

We have presented a simple, effective, and Bio-MEMS compatible technique for patterning macrophage cells on gold/silicon substrates with prolonged cell selectivity. Two control surfaces, silicon with native and wet oxide, that are typically used in development of Bio-MEMS devices, were utilized for comparative studies throughout this investigation. Through extensive characterization of the surface properties, we established that a stable PEG coating is essential to achieving improved cell selectivity and that the prolonged PEG integrity in cell culture medium may be related to the presence of oxide states other than silicon dioxide on silicon substrates. Such an oxide surface might have served dual purposes: a relatively low affinity to proteins that suppresses the protein adsorption and a surface with favorable chemistry on which a stable PEG coating can be developed (Tables 1 and 2).

This study offers a new strategy for development of highly stable, cell-resistant surfaces, which can be significant in engineering stable and controllable material−biosystem interfaces and in developing Bio-MEMS devices, where biocompatibility is of major concern. The ability to pattern microarrays

of cells makes statistical analysis of cell behavior possible. The cell patterning with high selectivity and biostability facilitates development of a variety of biomedical devices for clinical monitoring, food industry, lab-on-a-chip diagnosis and analysis systems, and other health care services.

Acknowledgment. The authors thank the University of Washington Engineered Biomaterials (UWEB) Research Center for the partial financial support (NSF-EEC 9529161) and the lab assistance from Joyce Tseng, Omid Veiseh, Lisamarie Ramos, Yumiko Kusuma, and Ryan T. Kosai. Also acknowledged is the Surface Analysis Center for Biomedical Problems (NESAC/BIO-NIH Grant EB-002027) and the assistance of Dr. Lara Gamble for surface characterization by ESCA, and UWEB optical microscopy and image analysis shared resource, funded by the National Science Foundation (Grants EEC-9872882 and EEC-9529161).

JA055473Q